

## **A FOUR-PARAMETER M-PROFILE MODEL FOR THE EVAPORATION DUCT ESTIMATION FROM RADAR CLUTTER**

**J.-P. Zhang and Z.-S. Wu**

School of Science  
Xidian University, Xi'an 710071, China

**Q.-L. Zhu and B. Wang**

China Research Institute of Radio Wave Propagation  
Qingdao 266107, China

**Abstract**—A new four-parameter modified refractivity profile (M-profile) model for the evaporation duct is introduced in this paper. In the estimation of radio refractivity structure from sea clutters, a parametric M-profile model is normally employed. The conventional M-profile model for evaporation ducts is the one-parameter log linear model, which has some potential disadvantages in describing the observed M-profiles which would result in rough results of evaporation duct estimation. Based on this model, three new parameters are introduced and a four-parameter M-profile model is proposed here. This model has the ability to (a) more accurately match real-world M-profiles, (b) well replicate the observed clutter field, and (c) show clutter power or path loss sensitivity to each model parameter. All these abilities are necessary for robust refractivity estimations. The performance of this model is tested and validated through the estimation for two truly measured M-profiles.

### **1. INTRODUCTION**

The evaporation duct created by a rapid decrease of moisture immediately above the ocean surface is a quasi-permanent phenomenon. For microwaves at frequencies above L-band, the evaporation duct is the dominant propagation mechanism resulting in over-the-horizon radar detection or making radar holes appear. Many effects of the oceanic

evaporation duct on radar signals are investigated by Anderson [1], Woods et al. [2], Hitney and Vieth [3], and Paulus [4].

Without the consideration of other influencing factors such as rainfall [5], the propagation of electromagnetic waves in the atmosphere is mainly determined by the structures of the refractive index [6], so propagation models (e.g., the terrain parabolic equation model (TPEM)) require a refractivity profile to make their calculations. The description capability of the profile affects the calculation precision significantly. For operational uses, the modified refractivity profile (M-profile) is preferred. In the M-profile for the evaporation duct, the height where the profile reaches its minimum value and the modified refractivity gradient is zero is a critical parameter for characterizing the profile and is called the evaporation duct height. There are various models to determine the evaporation duct height, such as the Paulus-Jeske (P-J) model, Musson-Genon-Gauthier-Burth (MGB) model, and Babin model [7]. All these models involve finding an expression for the vertical refractivity gradient in terms of atmospheric variables from bulk meteorological measurements and the Monin-Obukhov similarity theory which is used to the surface layer.

A promising method for quantifying refractivity structures in near real time is based on inference from radar sea clutters, which was carried out successfully by Rogers et al. [8] and Gerstoft et al. [9]. The estimation or inference of the refractivity profile from clutter is an inverse problem, so it must be based on a parametric environmental model which affects the estimation precision significantly. For evaporation ducts, such a model is the log linear vertical M-profile model given by Paulus [4,10], which is determined only by the evaporation duct height and has been used successfully in a number of applications [8,11]. However, it has some potential disadvantages in describing real-world refractivity profiles, which are illustrated in Section 2. We introduce three new parameters into the log linear model to improve the profile description capability and the estimation precision of the actual M-profile. The new model is referred to as the “four-parameter model” here.

## 2. CONVENTIONAL M-PROFILE MODEL

### 2.1. Formulation

The propagation of microwaves in low levels of troposphere depends on vertical profiles of modified refractivity. Paulus [10] developed the following M-profile formula for evaporation ducts in a manner similar

to Jeske [12].

$$M(z) = M_0 + 0.125z - 0.125 \frac{\delta + z_0}{\phi(\delta/L')} \int_0^z \frac{\phi(z/L')}{z + z_0} dz, \quad (1)$$

where  $z$  is height in meters,  $z_0$  is the aerodynamic roughness length,  $\delta$  is evaporation duct height in meters,  $M_0$  is the modified refractivity at the sea surface,  $L'$  is the Monin-Obukhov scaling length corrected for stability, and  $\phi(z/L')$  is a stability-dependent function.

For different thermal conditions, Equation (1) has different forms. Assuming neutral conditions, Paulus [4, 10] presented a one-parameter log linear formula for evaporation ducts as follows:

$$M(z) = M_0 + 0.125z - 0.125\delta \ln[(z + z_0)/z_0], \quad (2)$$

where  $z_0$  is taken to be  $1.5 \times 10^{-4}$  m. This formula, although only accounting for the neutral conditions, is commonly used as the conventional model to describe the evaporation duct M-profile in all environments.

## 2.2. Disadvantages

In most cases, Equation (2) is known to be a reasonable approximation of the M-profile for the evaporation duct, and it usually can describe many actual M-profiles in the surface layer of marine atmosphere, yet this model has some potential disadvantages as follows.

1) Using only the evaporation duct height to describe the actual surface layer environment is a limitation. Note that the M-deficit (the difference between the minimum value of modified refractivity and its value at the sea surface) of the trapping layer and the duct height are one-to-one correspondence in (2), i.e., the M-deficit is fixed for a certain duct height, which is unrealistic for many cases (e.g., the experimental profiles shown in Figure 1 by Goldhirsh and Dockery [13] and Figure 4 by Gerstoft et al. [14]).

For physical considerations, this problem can be illustrated through the atmosphere stability conditions. Equation (2) assumes thermally neutral conditions and thus does not account for stability effects on the shape of the profile. In the open ocean where unstable conditions are more common, this formula is unreasonable. The Monin-Obukhov length  $L'$  is often used for the stability criterion, which is negative under unstable atmospheric stratification and positive under stable stratification and its magnitude typically ranges from a few meters to hundreds of meters. For neutral conditions, its absolute value is very large or even infinite.

One set of M-profiles for evaporation ducts with the same duct height but for different stability conditions is shown in Figure 1. It

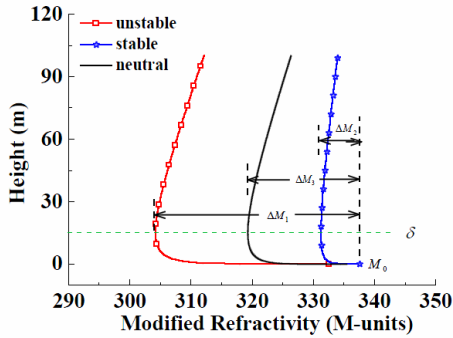


**Figure 1.** M-profiles for evaporation ducts in different stability conditions. The duct height  $\delta = 15$  m. The profiles for unstable, neutral, and stable conditions are with  $L' = -50$ ,  $L' = 1.0e5$ , and  $L' = 50$ , respectively.

is obvious that the M-deficits, which are defined as the evaporation duct strength  $\Delta M$  here, are different for profiles in unstable, neutral, and stable conditions, even with the same duct height. The same phenomenon was exploited by Paulus and Anderson [15], in which it was pointed out that the neutral profile and the unstable profile have nearly the same shape except for the difference in gradient in the very lowest levels of the profiles. This difference in gradient corresponds to the difference in  $\Delta M$ . Therefore, the duct strength  $\Delta M$  should be considered and parameterized. Douvenot et al. [16] also pointed out the limitation of only using the duct height, in his work of duct parameters inversion.

2) The changing rate of the gradient of modified refractivity (i.e., the second derivative of  $M$  in the vertical direction) between the sea surface level and the evaporation duct height level is determined by  $\delta$ , for which the model cannot describe profiles whose height gradients change more quickly or slowly, at the duct height level especially. Examples are shown in Figures 2 and 4(a), (b).

3) Above the evaporation duct height, the gradient of  $M$  is always concentrated around 0.125 M-units/m as the height increases. In many cases, the modeled profiles are inconsistent with the observed refractivity profiles in these levels, as shown in Figure 4.

4) The profiles described by this one-parameter model have very long tails in the very lowest height levels (see Figure 4), i.e., the modified refractivity near the surface varies very fast by logarithmic law, leading to anomalously high gradients of  $M$ , which cause deflections of radio waves to large angles from the horizontal direction and preclude propagation to large distances [17]. Therefore, the

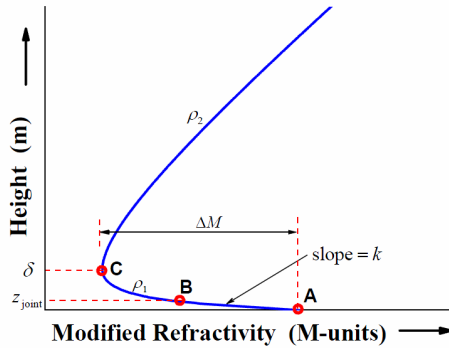


**Figure 2.** Four-parameter vertical M-profile for an evaporation duct.

logarithmic law is potentially no longer fulfilled at very small heights. Mabey [18] pointed out that the experimental data (kite and buoy data collected in the Roughness and Evaporation Duct experiment) did not show strong gradients of the modified refractivity just above the surface that were expected from theory. In Refs. [17, 19], it was shown that the approximation of the vertical profile at a height of less than 2 m by a tangent straight line is quite good.

Because of these potential disadvantages, the log linear model can not describe many real-world M-profiles and some actual vertical M-profiles for evaporation ducts can not be estimated precisely. A four-parameter M-profile model will be introduced in the next section.

### 3. FOUR-PARAMETER M-PROFILE MODEL

The changing rate of the gradient of modified refractivity given by (2) is

$$d^2M/dz^2 = 0.125\delta/(z + z_0)^2. \tag{3}$$

Considering the second disadvantage given in Section 2.2, in order to make this changing rate adjustable, an adjustment factor  $\rho_1$  ( $\rho_1 > 0$ ) is introduced to the right side of (2) in the following manner:

$$M(z) = M_0 + 0.125\rho_1 \{z - \delta \ln[(z + z_0)/z_0]\}. \tag{4}$$

Note that the height behavior of modified refractivity formulated by (4) is only used to describe M-profiles lower than the evaporation duct height  $\delta$ .

For the fourth disadvantage, we use a linear function to formulate the profile at heights lower than a certain level,  $z_{\text{joint}}$ . Different from the method in Ref. [19], this certain height is not fixed at 2 m but determined by the slope continuity of the profile curve. As shown in

Figure 2, the line AB with slope  $k$  ( $k \leq 0$ ) in the vertical direction is the substitute for the log linear M-profile described by (4) at heights lower than  $z_{\text{joint}}$ . Let the slope of the modified refractivity profile given by (4) with respect to height equal the slope of AB as follows:

$$\frac{dM}{dz} = 0.125\rho_1 \left( 1 - \frac{\delta}{z + z_0} \right) = k, \tag{5}$$

we can get

$$z = \frac{\delta}{1 - 8k/\rho_1} - z_0, \quad k \leq 0 \tag{6}$$

where  $z$  is the height where the segment AB and BC of the profile connect smoothly, labeled  $z_{\text{joint}}$  here. The modified refractivity as a function of height for evaporation ducts at heights lower than  $z_{\text{joint}}$  (the line AB in Figure 2) is given by

$$M(z) = M_0 + kz, \quad z \leq z_{\text{joint}} \tag{7}$$

For the height interval between  $z_{\text{joint}}$  and  $\delta$ , the M-profile is formulated by (4) with an offset  $M_1^{\text{offset}}$  added as follows:

$$\begin{aligned} M(z) &= M_0 + M_1^{\text{offset}} + 0.125\rho_1 z - 0.125\rho_1 \delta \ln[(z + z_0)/z_0] \\ &= M_0 + (k - 0.125\rho_1)z_{\text{joint}} + 0.125\rho_1 z + 0.125\rho_1 \delta \ln\left(\frac{z_{\text{joint}} + z_0}{z + z_0}\right), \\ & \hspace{15em} z_{\text{joint}} < z < \delta \tag{8} \end{aligned}$$

with

$$\begin{aligned} M_1^{\text{offset}} &= (M_0 + kz_{\text{joint}}) - (M_0 + 0.125\rho_1 z_{\text{joint}} \\ & \quad - 0.125\rho_1 \delta \ln [(z_{\text{joint}} + z_0)/z_0]) \\ &= (k - 0.125\rho_1)z_{\text{joint}} + 0.125\rho_1 \delta \ln [(z_{\text{joint}} + z_0)/z_0] \end{aligned}$$

This offset is used to make the modified refractivity given by (4) and (7) have the same value at  $z_{\text{joint}}$ , i.e., it ensures the geometrical continuity of segments AB and BC of the profile.

Considering the third disadvantage, in order to make the gradients of  $M$  at levels higher than  $\delta$  adjustable, a gradient adjustment factor  $\rho_2$  ( $\rho_2 > 0$ ) is introduced into the log linear M-profile model as follows:

$$M(z) = M_0 + 0.125\rho_2 z - 0.125\rho_2 \delta \ln [(z + z_0)/z_0]. \tag{9}$$

The M-profile at levels higher than the evaporation duct height  $\delta$  is formulated using (9) with another offset  $M_2^{\text{offset}}$  added, which ensures the continuity of  $M$  at  $\delta$ .

$$\begin{aligned} M(z) &= M_0 + M_2^{\text{offset}} + 0.125\rho_2 z - 0.125\rho_2 \delta \ln [(z + z_0)/z_0] \\ &= M_0 + (k - 0.125\rho_1)z_{\text{joint}} + 0.125(\rho_1 - \rho_2)\delta \\ & \quad + 0.125\rho_2 z + 0.125\delta \ln \left[ \frac{(z_{\text{joint}} + z_0)^{\rho_1}}{(\delta + z_0)^{\rho_1 - \rho_2} \cdot (z + z_0)^{\rho_2}} \right], \quad z \geq \delta \tag{10} \end{aligned}$$

with

$$\begin{aligned}
 M_2^{\text{offset}} &= \left[ M_0 + (k - 0.125\rho_1)z_{\text{joint}} + 0.125\rho_1\delta + 0.125\rho_1\delta \ln\left(\frac{z_{\text{joint}} + z_0}{\delta + z_0}\right) \right] \\
 &\quad - \{M_0 + 0.125\rho_2\delta - 0.125\rho_2\delta \ln[(\delta + z_0)/z_0]\} \\
 &= (k - 0.125\rho_1)z_{\text{joint}} + 0.125(\rho_1 - \rho_2)\delta \\
 &\quad + 0.125\delta \ln \left[ \frac{(z_{\text{joint}} + z_0)^{\rho_1}}{(\delta + z_0)^{\rho_1 - \rho_2} \cdot z_0^{\rho_2}} \right]
 \end{aligned}$$

It is noteworthy to point out that the slopes of two profile segments given by (8) and (10) have the same value at height  $\delta - z_0$ , which ensures the slope continuity of the profile.

The evaporation duct strength  $\Delta M$  of the new modeled M-profile is

$$\begin{aligned}
 \Delta M &= M_A - M_C \\
 &= M_0 - \left\{ M_0 + (k - 0.125\rho_1)z_{\text{joint}} + 0.125(\rho_1 - \rho_2)\delta \right. \\
 &\quad \left. + 0.125\rho_2\delta + 0.125\delta \ln \left[ \frac{(z_{\text{joint}} + z_0)^{\rho_1}}{(\delta + z_0)^{\rho_1 - \rho_2} \cdot (\delta + z_0)^{\rho_2}} \right] \right\} \\
 &= (0.125\rho_1 - k)z_{\text{joint}} - 0.125\rho_1\delta - 0.125\rho_1\delta \ln \left[ \frac{z_{\text{joint}} + z_0}{\delta + z_0} \right] \quad (11)
 \end{aligned}$$

Upon substituting the expression of  $z_{\text{joint}}$  given by (6) into (11) and simplifying, we obtain

$$\begin{aligned}
 \Delta M &= (0.125\rho_1 - k) \left( \frac{\delta}{1 - 8k/\rho_1} - z_0 \right) \\
 &\quad + 0.125\rho_1\delta \ln [(\delta + z_0)(1 - 8k/\rho_1)/e\delta], \quad (12)
 \end{aligned}$$

which is an implicit expression of the slope  $k$  that must be used in the profile description.

Equations (6), (7), (8), (10) and (12) are the formulation of the four-parameter M-profile model for evaporation ducts. It is parametric in evaporation duct height (EDH)  $\delta$ , evaporation duct strength (EDS)  $\Delta M$ , the  $M$  gradient adjustment factor  $\rho_1$  and  $\rho_2$  for profile segments at levels lower and higher than  $\delta$ , respectively.

## 4. PERFORMANCE AND VALUE VALIDATION

### 4.1. Advantages

The three new introduced parameters are used to account for the disadvantages in Section 2, so the four-parameter model can describe

the M-profile more freely than the log linear model does. The effects of  $\Delta M$ ,  $\rho_1$  and  $\rho_2$ , along with the conventional parameter  $\delta$ , on the shape of the profile are shown in Figure 3. The role of each parameter in determining the profile can be seen easily. Note that although  $\rho_1$  affects the profile in a small scale, yet the small change in these height levels where  $\rho_1$  works introduces great influence on wave propagation.

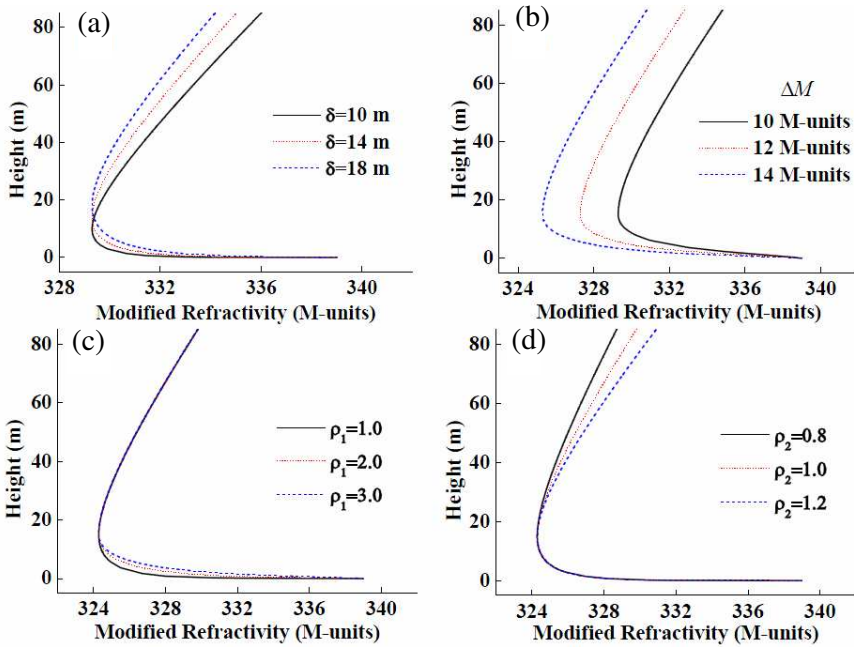


**Figure 3.** Roles of four parameters in describing vertical M-profiles. (a)  $\Delta M = 10$  M-units,  $\rho_1 = 1.0$ ,  $\rho_2 = 1.0$ , (b)  $\delta = 15$  m,  $\rho_1 = 3.0$ ,  $\rho_2 = 1.0$ , (c)  $\delta = 15$  m,  $\Delta M = 15$  M-units,  $\rho_2 = 1.0$ , (d)  $\delta = 15$  m,  $\Delta M = 15$  M-units,  $\rho_1 = 1.0$ .

To get a better estimation of the evaporation duct from radar sea clutter, two advantages and one necessary property of this four-parameter model should be validated: the ability to (a) more accurately match real-world M-profiles, (b) replicate the observed clutter field, and (c) show clutter power or path loss sensitivity to each model parameter. Only when all these aspects are validated can robust estimation results be expected. The M-profile matching ability is illustrated in Figure 4. Note that the log linear model and the four-parameter model use the same evaporation duct height in each case. Obviously, the four-parameter model is more robust in matching the observed M-profiles through choosing appropriate parameter values.

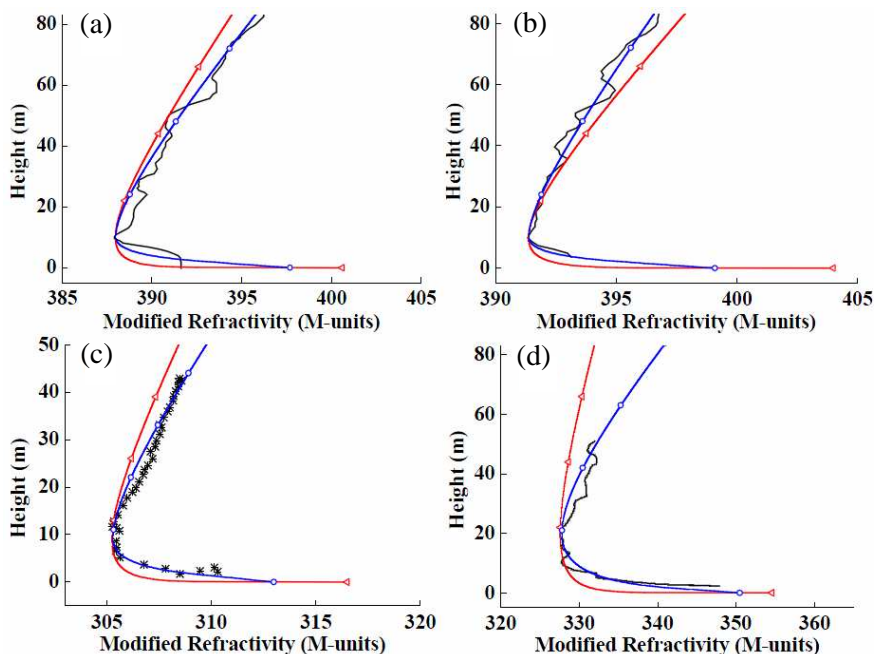


**Figure 4.** Measured and modeled vertical M-profiles. The red line with triangles represents the M-profile based on the log linear model. The blue line with circles represents the M-profile based on the four-parameter model. The black lines or asterisks represent the measured M-profiles from (a)–(b) [20], (c) [21], and (d) [22]. The profiles based on the two models are described with: (a)  $\delta = 10$  m,  $\Delta M = 10$  M-units,  $\rho_1 = 4.9$ ,  $\rho_2 = 1.2$ , (b)  $\delta = 10$  m,  $\Delta M = 8$  M-units,  $\rho_1 = 4.0$ ,  $\rho_2 = 0.8$ , (c)  $\delta = 9$  m,  $\Delta M = 8$  M-units,  $\rho_1 = 4.0$ ,  $\rho_2 = 1.4$ , and (d)  $\delta = 20$  m,  $\Delta M = 23$  M-units,  $\rho_1 = 3.5$ ,  $\rho_2 = 3.0$ .

Although these comparisons are limited in number, yet do serve to illustrate its advancement in M-profile descriptions.

The validation of the replicated clutter field is based on an example of observed clutter [22] shown in Figure 5. The corresponding refractivity environment is of the vertical M-profile shown in Figure 4(d). We can see that the observed clutter has a very complex constructive/destructive interference. According to this interference pattern, the modeled clutter (note that the surface scattering theories are used in the modeling [23–25]) based on the four-parameter refractivity profile matches the observed clutter better than that based on the log linear profile. The clutter from the log linear M-profile very poorly matches the observed clutter power. The discrepancy between the blue line and the black line in ranges

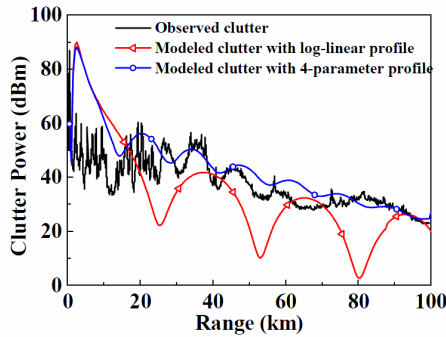


**Figure 5.** Observed and modeled clutters versus range for the atmospheric refractive structure shown in Figure 4(d).

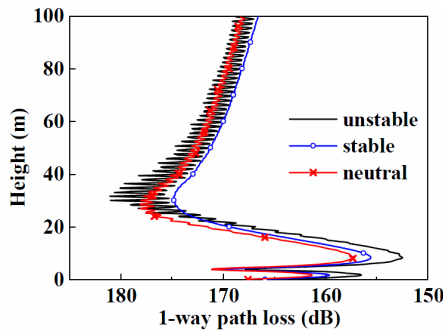


**Figure 6.** Simulated path loss at 80 km based on the four-parameter M-profile model. The unstable, stable, and neutral conditions are accounted for by  $L' = -100, 100,$  and  $1.0e5$ , corresponding to  $\Delta M = 42.9, 13.2,$  and  $27.0$  M-units, respectively.  $\delta = 20$  m,  $\rho_1 = 2.0,$   $\rho_2 = 1.0$ .

larger than 60 km is probably due to range dependencies of the true refractivity field.

As depicted in Section 2.2, the atmospheric stability can be accounted for by the duct strength  $\Delta M$ . In order to illustrate the path loss performance based on the four-parameter model under different thermal conditions, Figure 6 shows a test of it in three environments. The radar parameters for this test are shown in Table 1, and the wind speed is 10 m/s. We can see that the path losses under different conditions are different, indicating the four-parameter model can account for different thermal stabilities. The effects of other three parameters on the path loss performance are also tested as shown in Figure 7. Clearly, a small change in the modeled vertical profile can introduce a great change in the path loss, so all the three added parameters along with  $\delta$  are valid and valuable for propagation

Table 1. Radar parameters.

Parameter	Value (Units)
Frequency	10 GHz
Beam width	0.7°
Antenna height	13 m
Polarization	HH

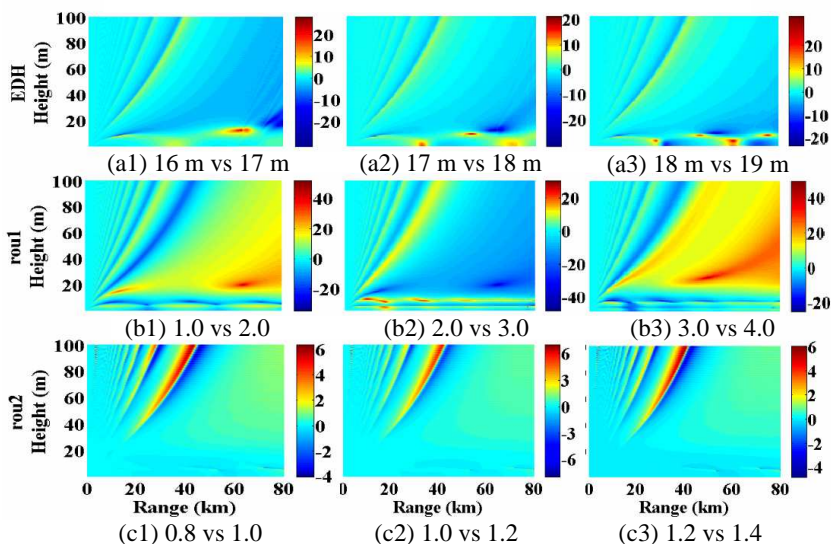
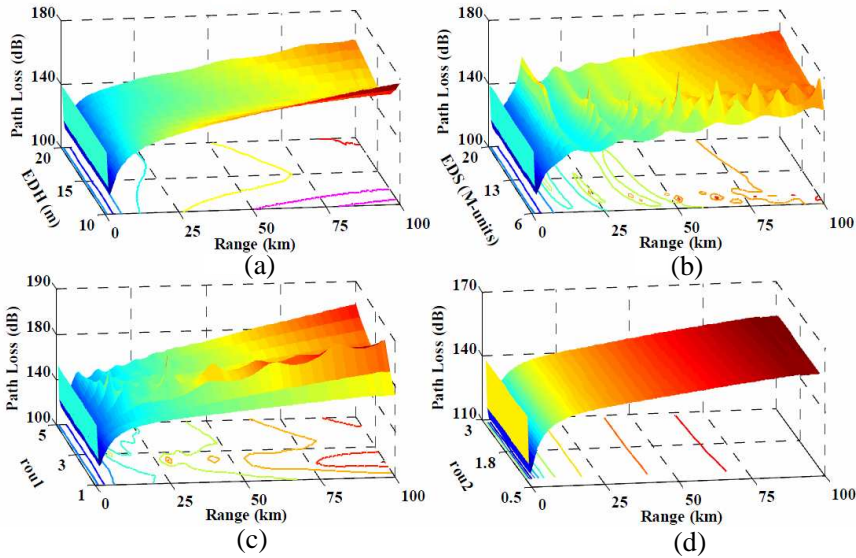


Figure 7. Relative change (dB) in path loss between two coverage diagrams based on the four-parameter model with two neighboring values (above each subfigure) of each parameter. For example, subfigure (a1) plots the change between the coverage diagram calculated with the EDH 16 m and that calculated with EDH 17 m. Other parameters are taken here as (a1)–(a3)  $\Delta M = 15$  M-units,  $\rho_1 = \rho_2 = 1.0$ , (b1)–(b3)  $\delta = 20$  m,  $\Delta M = 20$  M-units,  $\rho_2 = 1.0$ , (c1)–(c3)  $\delta = 20$  m,  $\Delta M = 20$  M-units,  $\rho_1 = 1.0$ .

calculations, and the new model is better than the conventional model in this meaning.

#### 4.2. Path Loss Sensitivity to Model Parameters

The path loss sensitivity to each of the model’s new parameters must also be validated to ensure it’s feasibility for estimating refractivity



**Figure 8.** Path loss sensitivity to each model parameter. Other parameters are taken here as (a)  $\Delta M = 10$  M-units,  $\rho_1 = \rho_2 = 1.0$ , (b)  $\delta = 15$  m,  $\rho_1 = 3.0$ ,  $\rho_2 = 1.0$ , (c)  $\delta = 15$  m,  $\Delta M = 15$  M-units,  $\rho_2 = 1.0$ , (d)  $\delta = 15$  m,  $\Delta M = 15$  M-units,  $\rho_1 = 1.0$ .

structures robustly from sea clutter. An example of this sensitivity is shown in Figure 8. The path losses are calculated using the parabolic equation method with radar parameters shown in Table 1. The antenna height is 7 m. Because the input information for the estimation is the observed sea clutter at the effective scattering height of the sea surface, the path loss is calculated at the corresponding height (assumed to be 1.0 m here). According to the path loss contours, it is clear that the path loss is sensitive to EDH  $\delta$ , EDS  $\Delta M$ , and  $\rho_1$ , but is not sensitive to  $\rho_2$ . The path loss hardly changes as  $\rho_2$  varies. That is because  $\rho_2$  is a parameter affecting  $M$  gradients at levels higher than EDH, and the  $M$  gradients at these levels have little influence on path losses at levels lower than EDH. However, this parameter is still valuable because it is used to model the  $M$ -profile at levels higher than EDH and the path losses at these levels are sensitive to it, which can be seen from Figures 7(c1)–(c3).

Consequently, for evaporation duct estimation from sea clutter,  $\delta$ ,  $\Delta M$  and  $\rho_1$  can be retrieved using their path loss sensitivity, and the inversion for  $\rho_2$  can adopt the information of path losses or meteorology at levels higher than EDH.

### 4.3. Evaporation Duct Estimation Results and Discussion

We use two measured M-profiles to test the performance of the four-parameter model in evaporation duct estimation. The radar parameters are the same with those used in Figure 8. For comparison, the estimation is performed with the four-parameter model and the log linear model respectively, and the results are shown in Figure 9 simultaneously. The least squares error function is used as the objective function to calculate the match between the modeled and observed

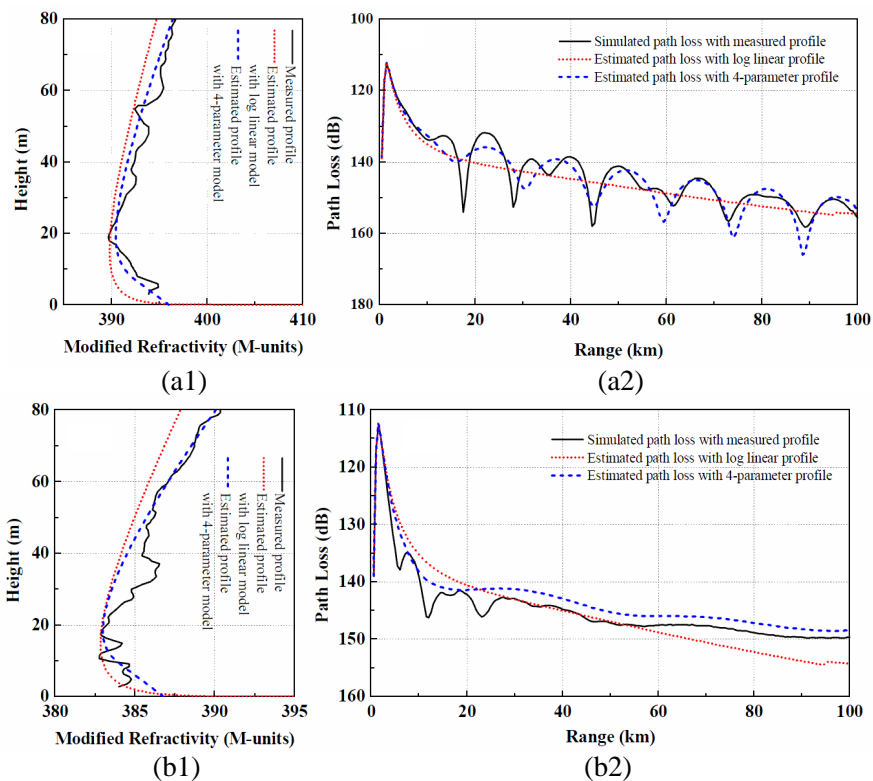


**Figure 9.** Estimated results for two measured M-profiles. The retrieved parameter values for cases (a1) and (b1) are: (log linear profile)  $\delta = 15.35$  m; (4-parameter profile)  $\delta = 18.76$  m,  $\Delta M = 5.85$  M-units,  $\rho_1 = 2.46$ ,  $\rho_2 = 1.40$ , and (log linear profile)  $\delta = 14.91$  m; (4-parameter profile)  $\delta = 18.02$  m,  $\Delta M = 4.05$  M-units,  $\rho_1 = 2.57$ ,  $\rho_2 = 1.61$ , respectively.  $\rho_2$  is chosen here according the profile match, since there are no path loss information at levels higher than EDH. The associated path losses calculated with the retrieved parameters are plotted in (a2) and (b2).

clutters, and it is optimized by PSO [26] in the estimation with the four-parameter model. Because there is only one parameter in the log linear model, the exhaustive search is used in the estimation with this model. All inversions are carried out on the one-way path losses simulated with the measured M-profiles.

As shown in Figures 9(a1) and (b1), the estimated profiles with the four-parameter model are more close to the measured profiles, illustrating the stronger ability of the new model in evaporation duct estimation. The path losses corresponding to each estimated profile are plotted in Figures 9(a2) and (b2). Obviously, the original path losses simulated with the measured M-profiles are more accurately replicated when the 4-parameter profiles are used as the refractivity structures. This is also a further validation of the new model's ability (b) described in Section 4.1.

## 5. CONCLUSIONS

A four-parameter vertical M-profile model for the evaporation duct estimation from radar sea clutter is introduced. It has advantages in matching real-world modified refractivity profiles and in serving as the environmental model for the propagation calculation and refractivity estimation. In order to apply this model to evaporation duct estimation from radar sea clutters, the path loss sensitivity to each model parameter is analyzed and the results show that these four new parameters are valid and valuable for the robust estimation. Through the test of estimating two truly measured M-profiles, it is concluded that the measured profile will be more accurately retrieved when the new model with these four parameters is employed.

## ACKNOWLEDGMENT

This research was supported by the National Natural Science Foundation of China (Nos. 60771038 and 60971065).

## REFERENCES

1. Anderson, K. D., "Radar measurements at 16.5 GHz in the oceanic evaporation duct," *IEEE Trans. Antennas Propag.*, Vol. 37, No. 1, 100–106, 1989.
2. Woods, G., A. Ruxton, C. Huddleston-Holmes, and G. Gigan, "High-capacity, long-range, over ocean microwave link using the evaporation duct," *IEEE J. Ocean. Eng.*, Vol. 34, No. 3, 323–329, 2009.

3. Hitney, H. V. and R. Vieth, "Statistical assessment of evaporation duct propagation," *IEEE Trans. Antennas Propag.*, Vol. 38, No. 6, 794–799, 1990.
4. Paulus, R. A., "Evaporation duct effects on sea clutter," *IEEE Trans. Antennas Propag.*, Vol. 38, No. 11, 1765–1771, 1990.
5. Meng, Y. S., Y. H. Lee, and B. C. Ng, "Further study of rainfall effect on VHF forested radio-wave propagation with four-layered model," *Progress In Electromagnetics Research*, Vol. 99, 149–161, 2009.
6. Alexopoulos, A., "Effect of atmospheric propagation in RCS predictions," *Progress In Electromagnetics Research*, Vol. 101, 277–290, 2010.
7. Babin, S. M., G. S. Young, and J. A. Carton, "A new model of the oceanic evaporation duct," *J. Appl. Meteorology*, Vol. 36, 193–204, 1997.
8. Rogers, L. T., C. P. Hattan, and J. K. Stapleton, "Estimating evaporation duct heights from radar sea echo," *Radio Sci.*, Vol. 35, No. 4, 955–966, 2000.
9. Gerstoft, P., L. T. Rogers, J. L. Krolik, and W. S. Hodgkiss, "Inversion for refractivity parameters from radar sea clutter," *Radio Sci.*, Vol. 38, No. 3, 8053, 2003.
10. Paulus, R. A., "Specification for environmental measurements to assess radar sensors," Tech. Rep. 1685, Naval Ocean Systems Center, San Diego, CA, Nov. 1989.
11. Yardim, C., P. Gerstoft, and W. S. Hodgkiss, "Sensitivity analysis and performance estimation of refractivity from clutter techniques," *Radio Sci.*, Vol. 44, 1008, 2009.
12. Jeske, H., "State and limits of prediction methods of radar wave propagation conditions over the sea," *Modern Topics in Microwave Propagation and Air-Sea Interaction*, A. Zancla (ed.), D. Reidel Publishing, 130–148, 1973.
13. Goldhirsh, J. and G. D. Dockery, "Measurement resolution criteria for assessment of coastal ducting," *Proc. 9th Int. Conf. Antennas and Propagation*, 317–322, 1995.
14. Gerstoft, P., W. S. Hodgkiss, L. T. Rogers, and M. Jablecki, "Probability distribution of low altitude propagation loss from radar sea clutter data," *Radio Sci.*, Vol. 39, 6006, 2004.
15. Paulus, R. A. and K. D. Anderson, "Application of an evaporation duct climatology in the littoral," *Battle Space Atmospheric and Cloud Impact on Military Oper. Conf.*, Fort Collins, CO, 1990.
16. Douvenot, R., V. Fabbro, C. Bourlier, J. Saillard, H. Fuchs,

- H. Essen, et al., "Retrieve the evaporation duct height by least-squares support vector machine algorithm," *J. Appl. Remote Sens.*, Vol. 3, 1–15, 2009.
17. Ivanov, V. K., V. N. Shalyapin, and Y. V. Levadny, "Microwave scattering by tropospheric fluctuations in an evaporation duct," *Radiophysics and Quantum Electronics*, Vol. 52, No. 4, 277–286, 2009.
  18. Mabey, D. L., "Variability of refractivity in the surface layer," M.S. Thesis, Naval Postgraduate School, Monterey, CA, 2002.
  19. Bocharov, V. G., A. V. Kukushkin, V. G. Sinitsyn, and I. M. Fuks, "Propagation of radio waves in tropospheric evaporation ducts," *Inst. Radiophys. Electron., National Acad. Sci.*, No. 126, Kharkov, Ukraine, Preprint, 1979.
  20. Wu, F., "The research of parabolic equation in the troposphere," M.S. Thesis, School of Science, Wuhan University of Technology, Wu Han, Hubei, 2008 (in Chinese).
  21. Wang, X.-M., "A study on the atmospheric duct over ocean and its prediction," M.S. Thesis, Remote Sensing College, Nanjing University of Information Science and Technology, Nanjing, Jiangsu, 2007 (in Chinese).
  22. Wang, B., Z.-S. Wu, Z. Zhao, and H.-G. Wang, "Retrieving evaporation duct heights from radar sea clutter using particle swarm optimization (PSO) algorithm," *Progress In Electromagnetics Research M*, Vol. 9, 79–91, 2009.
  23. Wu, Z.-S., J.-P. Zhang, L.-X. Guo, and P. Zhou, "An improved two-scale model with volume scattering for the dynamic ocean surface," *Progress In Electromagnetics Research*, Vol. 89, 39–56, 2009.
  24. Liang, D., P. Xu, L. Tsang, Z. Gui, and K.-S. Chen, "Electromagnetic scattering by rough surfaces with large heights and slopes with applications to microwave remote sensing of rough surface over layered media," *Progress In Electromagnetics Research*, Vol. 95, 199–218, 2009.
  25. Wang, A.-Q., L.-X. Guo, and C. Chai, "Numerical simulations of electromagnetic scattering from 2D rough surface: Geometric modeling by nurbs surface," *Journal of Electromagnetic Waves and Applications*, Vol. 24, No. 10, 1315–1328, 2010.
  26. Zhang, L., F. Yang, and A. Z. Elsherbeni, "On the use of random variables in particle swarm optimizations: A comparative study of Gaussian and uniform distributions," *Journal of Electromagnetic Waves and Applications*, Vol. 23, No. 5–6, 711–721, 2009.